

Determination of the Second Hydration Shell of Cr³⁺ and Zn²⁺ in Aqueous Solutions by Extended X-ray Absorption Fine Structure

Adela Muñoz-Páez,^{*,†} Rafael R. Pappalardo,[‡] and Enrique Sánchez Marcos[‡]

Contribution from the Departamento de Química Inorgánica e Instituto de Ciencia de Materiales, Facultad de Química, Universidad de Sevilla-CSIC, P.O. Box 553, 41012-Sevilla, Spain, and Departamento de Química Física, Facultad de Química, Universidad de Sevilla, 41012-Sevilla, Spain

Received June 8, 1995[⊗]

Abstract: The geometric structures of Cr(NO₃)₃ and Zn(NO₃)₂ aqueous solutions in a wide range of concentrations 2.7–0.005 *m* have been determined by means of the extended X-ray absorption fine structure (EXAFS) technique. X-ray absorption spectra at the K-edges of Zn and Cr have been measured in the transmission and fluorescence modes at the Synchrotron Radiation Source (U.K.). The analysis of all the experimental data (13 solutions) is compatible with a unique structural model, which basically agrees with the concentric shell model of Frank and Evans for ionic hydration. Therefore, it is shown that the EXAFS technique allows the determination of a second hydration shell in a wide range of concentrations, from almost saturated to highly dilute solutions. M–O distances (Cr–O_I = 2.00 Å, Zn–O_I = 2.05 Å) and the coordination number (6 for both cations) for the first hydration shell are not affected by concentration. A second hydration shell is detected in both cases, although for chromium solutions, this contribution to the EXAFS spectra is more important than for zinc. The distance is around 4.0 Å, but in Cr³⁺ solutions a slight increase in the Cr–O_{II} distance is observed with dilution (4.02 Å for 0.01 *m*, and 3.95 Å for 2.6 *m*). The Zn–O_{II} distance shows no systematic trend, the average distance being 4.1 Å. The coordination number for this shell is 13.3 ± 1 for Cr³⁺ solutions and 11.6 ± 1.6 for Zn²⁺ solutions. The most concentrated Zn²⁺ solution (2.7 *m*) presents a singular behavior, since its coordination number decreases to 6.8 ± 1.5. The data analysis procedure is thoroughly described, and the possibilities of an alternative hypothesis for the second contribution to the EXAFS spectrum, such as multiple scattering effects, are carefully discussed.

1. Introduction

Nowadays it is well recognized that a correct description of ionic solutions needs a precise knowledge of their geometrical structure. The reason for this is that consideration of the solvent as a dielectric continuum, into which the charged particles are embedded, does not give an accurate description of thermodynamic, dynamic, and transport phenomena in solutions.¹ Although electrostatic ion–solvent interactions are quite large and usually represent the most important contribution to the total interaction energy of the ionic solutions, physicochemical properties that depend on the structure of solvent molecules must usually be introduced into treatments of solutions, to achieve reasonable agreement with experiment. Thus, the different scales of empirical parameters of solvent polarity are useful tools to take into account explicitly specific solvent interactions.²

The experimental techniques giving substantial information about the structure of ionic solutions have been X-ray and neutron diffraction, which have become the most powerful techniques during the last 25 years. For almost all single ions in water, the structures of their solutions have been determined. Exhaustive reviews on this subject have recently been published by Marcus,^{3,4} Magini *et al.*,⁵ and Ohtaki *et al.*^{1,6} Apart from diffraction methods, during the last 15 years, the EXAFS

(extended X-ray absorption fine structure) technique has shown itself adequate for determining the geometrical structure of ionic solutions, partially due to the potential accessibility of this technique to deal with solutions 2 or 3 orders of magnitude more dilute than those studied by the diffraction techniques. This means, in principle, that EXAFS may be able to give information on highly dilute solutions (*ca.* 10⁻³ M) where the ion–solvent interactions are less disturbed by ion–ion interactions. Moreover, since the EXAFS technique is not limited by the concentration, the increasing role of the ion–ion interactions in determining the structure of the solution can be monitored by recording a set of EXAFS spectra corresponding to solutions of increasing concentration, eventually up to the saturated solutions. Thus, an increasing number of EXAFS papers of ionic solutions have appeared in the literature and have recently been reviewed by Ohtaki and Radnai.⁶ However, it has generally been considered that the sensitivity of the EXAFS to the disorder precluded the detection of the second hydration shell for cations^{1,5} by this technique. In a previous paper we have shown experimental evidence of the second hydration shell of Cr³⁺ in a 0.01 M aqueous solution of Cr(NO₃)₃.⁷ Likewise, Beagley and co-workers⁸ have published EXAFS spectra of MnCl₂ aqueous solutions where geometrical parameters for a second hydration shell were given for solutions of several

[†] Universidad de Sevilla-CSIC.

[‡] Universidad de Sevilla.

[⊗] Abstract published in *Advance ACS Abstracts*, November 15, 1995.

(1) Ohtaki, H. In *Structure and Dynamics of Solutions*; Ohtaki, H., Yamatera, H., Eds.; Elsevier: Amsterdam, 1992; Chapter 2.

(2) Reichardt, C. *Solvents and Solvent Effects in Organic Chemistry*, 2nd ed.; VCH: Weinheim, 1990.

(3) Marcus, Y. *Ion Solvation*; Wiley: Chichester, 1986.

(4) Marcus, Y. *Chem. Rev.* **1988**, *88*, 1475.

(5) Magini, M.; Licheri, G.; Paschina, G.; Piccaluga, G. *X-Ray Diffraction of Ions in Aqueous Solutions: Hydration and Complex Formation*; CRC Press: Boca Raton, FL, 1988.

(6) Ohtaki, H. and Radnai, T. *Chem. Rev.* **1993**, *93*, 1157.

(7) Muñoz-Páez, A.; Sánchez Marcos, E. *J. Am. Chem. Soc.* **1992**, *114*, 6931.

(8) Beagley, B.; McAuliffe, C. A.; Smith, S. P. B.; White, E. W. *J. Phys.: Condens. Matter* **1991**, *3*, 7919.

concentrations, 0.1M being the most dilute. More recently, Brewer *et al.*⁹ have modeled the EXAFS data of solutions of metal hexafluorides in anhydrous HF by a three-shell model that describes two fluoride coordination spheres around the metal. However, Sandström *et al.*¹⁰ have not found evidence of a second hydration sphere from EXAFS data of [Cr(H₂O)₆]³⁺ and [Rh(H₂O)₆]³⁺ in ca. 1 M aqueous solutions, where the existence of this shell has been well established by them, by means of other techniques such as large-angle X-ray scattering, neutron diffraction,¹¹ and double difference IR spectroscopy.¹² On the other hand, Sánchez del Río *et al.*¹³ have detected one peak in radial distribution function (RDF) at distances near that expected for a second hydration shell of a set of aqueous solutions of multicharged cations, but they ascribed the second contribution to multiple scattering effects inside the first hydration shell.

We present here a detailed study of two representative ions from the first transition period, Cr³⁺ and Zn²⁺, characterized by having quite different kinetic stabilities of their aquo complexes (the residence time of oxygen atoms of water molecules in the first hydration shell is 2×10^5 s for Cr³⁺,¹⁴ and less than 10^{-9} s for Zn²⁺¹⁵). A set of aqueous solutions of the nitrate salts of these two cations, with concentrations ranging from 0.005 to 2.7 *m* have been studied by EXAFS in order to examine the capability of this technique to supply structural information beyond the first hydration shell in a wide range of concentrations where dilute solutions are included. In this work we also present a set of experimental aspects of interest for measuring spectra of solutions, as well as the strategy used for data analysis.

2. Experimental Section

X-ray absorption spectroscopy (XAS) measurements were recorded at the K absorption edges of Cr and Zn (edge positions 5989 and 9659 eV, respectively) at the EXAFS station 8.1 (dipole radiation, focusing optics) of the Synchrotron Radiation Source (Daresbury Laboratory, U.K.) with a ring energy of 2 GeV and ring currents of 200 mA. This station operated with a double-crystal monochromator Si[220] which was detuned 30% in intensity for the chromium edge and 50% for the Zn edge, to minimize the presence of higher harmonics. Calibration of the monochromator was carried out using Cr and Zn foils. Resolution was estimated to be about 1.0 eV at the chromium edge by the sharp pre-edge peak of the spectrum of chromate ions, and 1.5 eV at the Zn edge by the small shoulder of the spectrum of Zn foil.

Measurements of the aqueous solutions were carried out at room temperature in the transmission and fluorescence modes, using different types of EXAFS liquid cells, depending on the type of experiment and the sample thickness required in each case to obtain the optimum absorption coefficient, $\mu x = 2.5$.

At the Cr K-edge, the absorption of water, the major component of the solutions, is comparable to that of chromium in medium and low concentrated solutions, the maximum path length being restricted for this reason. As a consequence, the lower concentrations cannot be measured accurately in the transmission mode because the change in the absorption coefficient at the Cr edge (step height) is too small; the amplitude of the EXAFS signal is then smaller than the noise amplitude.

According to Jacklevic and co-workers¹⁶ the fractional uncertainty in the measurement of the linear absorption coefficient of the solute element scales as $1/c_x$, c_x being the concentration of element x , in the transmission mode, while in fluorescence detection the scaling goes as $(1/c_x)^{1/2}$, giving this mode an advantage at lower concentrations. Using this expression the relative fractional uncertainty for a 0.1 *m* solution is 10/3.16 for the transmission/fluorescence modes. For the 0.01 *m* solution it scales to 100/10. Additional problems when using the fluorescence mode are sample and detector alignment and detector efficiency, which decrease the signal to noise ratio. Taking into account all these facts, 0.01 and 0.005 *m* solutions were measured in the fluorescence mode in a specially designed cell.¹⁷ The detector used was a Canberra 13-element high-purity germanium array, the output being fed via a shaping amplifier to a multichannel analyzer. The count rate in the fluorescence channel was 1400 counts/s below the edge and 25,000 counts/s above the edge. The depth of the liquid vein was 2.5 mm. Measurements of chromium nitrate solutions with concentrations of 2.6, 1.5, 0.1, and 0.05 *m* were carried out in the transmission mode, the path length for these samples being between 10 and 100 μ m. The cell used was a modified IR liquid cell, Specac 7500, with a variable path length, 0–7 mm. This cell was specially adapted for X-ray absorption measurements by substituting NaCl windows by a Teflon double O-ring, holding a Mylar film 25 μ m thick¹⁸ in the middle. The aperture of the O-ring was 13 mm in diameter.

For the Zn K-edge ($E = 9659$ eV) the absorption of water is negligible compared to that of Zn²⁺ ions. Therefore, the depth of the liquid vein can be increased considerably without significantly increasing the total absorption coefficient. In fact, the depth of pure water to have the optimum absorption, $\mu x = 2.5$, is 4.1 mm for this energy. This is particularly useful for the most dilute solutions. Thus, in the investigation of zinc solutions, the transmission mode, with another EXAFS liquid metal free cell,^{17,19} was used.

The solid samples of chromium and zinc crystalline hydrates were pressed into thin self-supporting wafers, adding boron nitride (BN) to bring the total absorbance to 2.5, and then measured in the transmission mode at 77 K under a He atmosphere.

Optimized ion chambers filled with the appropriate He/Ar mixture were used as detectors in all the transmission experiments. Each datum point was collected for 1 s and at least four scans were averaged, thus minimizing high- and low-frequency noise. To improve the signal to noise ratio, a higher number of scans were used in the most dilute solutions (up to 10 scans for 0.005 *m* Zn²⁺).

Water solutions were prepared by dissolving the desired amount of nitrate salts Cr(NO₃)₃·9H₂O and Zn(NO₃)₂·6H₂O supplied by Merck (reagent p.a.) in distilled water at the required pH to prevent hydrolysis²⁰ (pH ~1).

3. Data Analysis

The general expression for an EXAFS $\chi(k)$ function considering single scattering processes and plane wave approximation given by Stern *et al.*²¹ has been used. These functions for Cr and Zn K-edges were obtained from the X-ray absorption spectra by subtracting a Victoreen curve, which simulates the pre-edge absorption, followed by a cubic spline background removal.²² Normalization was performed by dividing by the height of the edge. E_0 was defined as the maximum in the first derivative of the absorption edge.

EXAFS parameters N (coordination number), $\Delta\sigma^2$ (Debye–Waller factor), R (coordination distance), and ΔE_0 (inner

(9) Brewer, S. A.; Brisdon, A. K.; Holloway, J. H.; Hope, E. G. *Polyhedron* **1994**, *13*, 749.

(10) Read, M. C.; Sandström, M. *Acta Chem. Scand.* **1992**, *46*, 1177.

(11) Broadbent, R. D.; Neilson, G. W.; Sandström, M. *J. Phys.: Condens. Matter* **1992**, *4*, 639.

(12) Bergström, P. A.; Lindgren, J.; Read, M.; Sandström, M. *J. Phys. Chem.* **1991**, *95*, 7650.

(13) Sánchez del Río, M.; García, J.; Burattini, E.; Benfatto, M.; Natoli, C. R. 2nd European Conference on Progress in X-ray Synchrotron Radiation Research. In *Conf. Proc. Vol. 25*; Balerna, A., Bernieri, E., Mobilio, S., Eds.; Società Italiana di Fisica: Bologna, 1990; p 35.

(14) Hunt, J.; Plane, R. A. *J. Am. Chem. Soc.* **1954**, *76*, 5960.

(15) Salmon, P. S.; Bellissent-Funel, M. C.; Herdman, G. J. *J. Phys.: Condens. Matter* **1990**, *2*, 4297.

(16) Jaklevic, J.; Kirby, J. A.; Klein, M. P.; Robertson, A. S.; Brown, G. S.; Eisenberger, P. *Solid State Commun.* **1977**, *23*, 679.

(17) Sánchez Marcos, E.; Gil, M.; Martínez, J. M.; Muñoz-Páez, A.; Sánchez Marcos, A. *Rev. Sci. Instrum.* **1994**, *65*, 2153.

(18) Villain, F.; Briois, V.; Castro, I.; Helary, C.; Verdager, M. *Anal. Chem.* **1993**, *65*, 2545.

(19) Muñoz-Páez, A.; Gil, M.; Martínez, J. M.; Sánchez Marcos, E. *Physica B* **1995**, *208–209*, 241.

(20) Sillen, L. G.; Martell, A. E. *Stability Constants of Metal-Ion Complexes*; Spec. Publ. Chem. Soc.: London, 1971; p 25.

(21) Stern, E. A.; Bunker, B. A.; Heald, S. M. *Phys. Rev. B* **1980**, *21*, 5521.

(22) Cook, J. W. Jr.; Sayers, D. E. *J. Appl. Phys.* **1981**, *52*, 5024.

potential correction) were obtained from EXAFS functions by nonlinear least squares fitting procedures using the program XDAP from the University of Eindhoven.²³ The phase shift and back-scattering amplitude functions characteristic for each type of neighboring atom have to be either derived theoretically, using the appropriate algorithms, or obtained from EXAFS spectra of compounds with known structure.²⁴ The successive algorithms proposed to calculate such functions^{25–27} have considerably improved its accuracy, making the data analysis carried out with them very reliable. Nevertheless, the values of some input parameters are needed to calculate these functions, such as the amplitude reduction factor, S_0^2 , and the Debye–Waller factor, σ . Since we did not have the values of these parameters for Cr–O and Zn–O contributions, we have obtained the phase shift and back-scattering amplitude functions for Cr–O from the EXAFS spectra of the crystalline hydrate $\text{Cr}(\text{NO}_3)_3 \cdot 9\text{H}_2\text{O}$ that presents a regular structure.²⁸ When studying metal ions in aqueous solutions, the corresponding hydrated crystals are generally considered good standards.²⁹ The corresponding crystalline zinc hydrate presents a distorted structure, with three different Zn–O distances between 2.064 and 2.130 Å in the first coordination shell,³⁰ which makes the experimental spectrum inappropriate to obtain the phase shift and back-scattering amplitude functions. For this reason, in this case we have obtained both functions, theoretically using the algorithm of Rehr *et al.*,²⁷ the FEFF program. As standard values, the amplitude reduction factor, S_0^2 , and Debye–Waller factor were set equal to 1 and 0, respectively, in the calculations of these functions. The suitability of the reference functions thus obtained was checked by using them in the fit of the solid crystalline hydrate.

When using experimental references, coordination numbers were corrected for the distance difference between the reference compound and the unknown according to³¹

$$N_{\text{cor}} = N e^{-2(R_{\text{ref}} - R_{\text{th}})/\lambda} \quad (1)$$

Errors in the structural parameters were calculated from the covariance matrix, taking into account statistical noise in the experimental EXAFS spectra and correlation between refined parameters. The quality of the fit is quantitatively expressed by means of the values of the goodness of fit (ϵ_v^2), calculated as outlined in the “Report on Standards and Criteria in EXAFS spectroscopy”:³²

$$\epsilon_v^2 = \frac{1}{v} \sum_{i=1}^{N_p} \frac{[\chi_i(\text{exptl}) - \chi_i(\text{model})]^2}{\sigma_i(\text{exptl})^2} \quad (2)$$

v = degrees of freedom and N_p = number of independent points.

(23) Vaarkamp, M.; Linders, J. C.; Koningsberger, D. C. *Physica B* **1995**, 208–209, 159.

(24) Vaarkamp, M. Ph.D. Thesis, Eindhoven University of Technology, Eindhoven, The Netherlands, 1993.

(25) Teo B. K.; Lee P. A. *J. Am. Chem. Soc.* **1979**, 111, 2815.

(26) McKale, A. G.; Veal, B. W.; Paulikas, A. P.; Chan, S. K.; Knapp, G. S. *J. Am. Chem. Soc.* **1988**, 110, 3763.

(27) Rehr, J. J.; Mustre de León, J.; Zabinsky, S. I.; Albers, R. C. *J. Am. Chem. Soc.* **1991**, 113, 5135.

(28) Kannan, K. K.; Viswamitra, M. A. *Acta Crystallogr.* **1965**, 19, 151.

(29) Sakane, H.; Miyayama, T.; Watanabe, I.; Yokoyama, Y. *Chem. Lett.* **1990**, 1623.

(30) Wyckhof, R. W. G. *Crystal Structure*; Interscience: New York, 1974.

(31) Kampers, F. W. H.; Engelen, C. W. R.; van Hooff, J. H. C.; Koningsberger, D. C. *J. Phys. Chem.* **1990**, 94, 8574.

(32) Lytle, F. W.; Sayers, D. E.; Stern, E. A. *Physica B* **1988**, 158, 701.

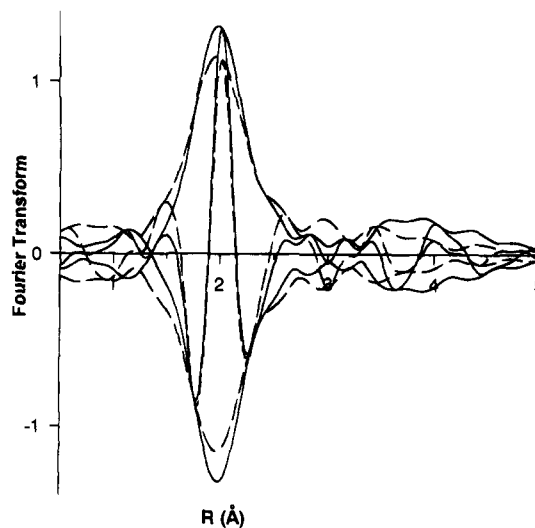


Figure 1. Phase-corrected Fourier transform of the EXAFS spectrum of Cr for a 0.1 *m* $\text{Cr}(\text{NO}_3)_3$ aqueous solution. k range analyzed: 2.77–12 Å⁻¹ (solid line), 3.54–12 Å⁻¹ (dashed line).

The range of the fitting process determines the number of independent points, N_p , in the spectrum, according to the Nyquist theorem,³³ $N_p = 2\Delta k\Delta R/\pi + 1$. The degrees of freedom, v , calculated by taking into account the number of fitting parameters, P , and the number of independent points, N_p ($v = N_p - P$), determine the goodness of fit (ϵ_v^2) values as outlined above.

The highest limit of the EXAFS function to be analyzed is basically determined by the signal/noise ratio. For ordered systems and high Z scatters, the back-scattering amplitude function decreases slowly with k , and thus for $k = 16$ Å⁻¹, the EXAFS function may have a considerable amplitude. Nevertheless, for disordered systems (*e.g.*, liquids) and for low Z scatterers (*e.g.*, oxygen atoms), the EXAFS signal can be negligible for $k \geq 12$ Å⁻¹. Moreover, for dilute systems the noise level increases rapidly. As a consequence, in the hydrated complexes here studied here, the maximum k values used are between 10 and 12 Å⁻¹.

The selection of the minimum k values of the EXAFS function investigated is more delicate in our case, particularly with that related to the detection of the second hydration shell. Taking into account that we are searching for M–O contributions in a liquid medium, both the amplitude function and the Debye–Waller factor should damp out the EXAFS signal rapidly. Thus, it is crucial to analyze the different components of $\chi(k)$ when they have the maximum intensity, *i.e.*, at low k values, particularly in the case of the hypothetical second hydration shell that should appear at a higher distance and, thus, will have a lower intensity. Consequently, special care was taken to select the value of the starting energy, which was kept in all cases as low as possible, *i.e.*, around 25 eV above the edge. The importance of this value is clearly shown in Figure 1, which includes the phase-corrected Fourier transform of the EXAFS spectrum of a Cr³⁺ solution, 0.1 *m*, taking two values for the minimum energy, the first and second nodes of the EXAFS spectrum, at 2.77 and 3.54 Å⁻¹, respectively (see below, Figure 3). A decrease in the range of the Fourier transform affects both the first peak, centered at 2.0 Å, and the second peak, centered at 4.0 Å, but while the first only decreases in intensity, the second nearly disappears. The possibility that the second peak is related to multiple scattering phenomena will be discussed in section 5.

(33) Brigham, E. O. *The Fast Fourier Transform*; Prentice Hall: Englewood Cliffs, NJ, 1974.

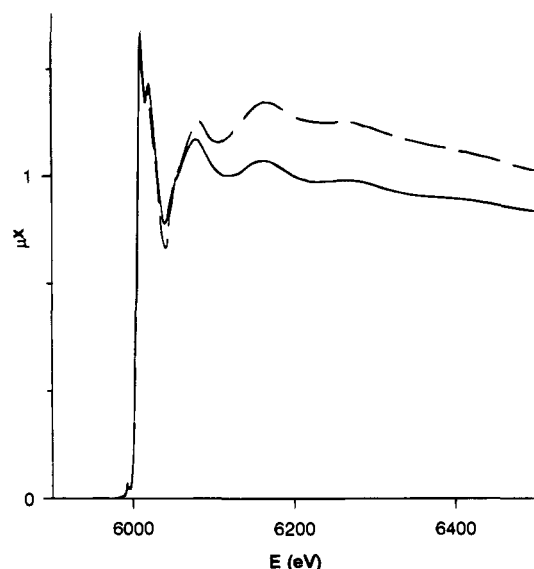


Figure 2. Normalized absorption spectrum at the Cr K-edge of the crystalline hydrate of $\text{Cr}(\text{NO}_3)_3$ (solid line) and the 0.1 *m* aqueous solution of the same salt (dashed line).

The noise amplitude (σ_i in eq 2) was estimated by averaging the raw absorption spectra obtained from several individual scans and by averaging the EXAFS functions, $\chi(k)$, of each individual scan, both methods yielding similar values. The advantages and drawbacks of fitting either the averaged $\chi(k)$ functions or a unique $\chi(k)$ function of the averaged raw data have been considered. The first option, although more tedious, has many advantages, as pointed out by some researchers.³⁴ In this option, the background subtraction can be optimized for each scan, and the noise amplitude is obtained from the variance of the different data sets used. Nevertheless, a small shift in the value of the edge position in one of the scans can cause a decrease in resolution of the final averaged EXAFS function. This problem can be avoided by averaging raw data that can be more accurately aligned by superimposing the sharp edge. For this reason we found the “classical” procedure, *i.e.*, averaging the raw data, determining the edge position, subtracting the background, and normalizing the obtained EXAFS spectra, more appropriate in our systems. Nevertheless, for chromium samples both methods have been followed, giving similar results, with only small differences in the values of the inner potential corrections obtained in the final fit ($\Delta E_0 \leq 1$ eV). The fitting results presented here correspond to the EXAFS function obtained by the classical method.

4. Results

4.1. Chromium solutions. Figure 2 shows the low-energy region of the normalized absorption spectrum at the Cr K-edge of the crystalline hydrate $\text{Cr}(\text{NO}_3)_3 \cdot 9\text{H}_2\text{O}$ and that of the 0.1 *m* $\text{Cr}(\text{NO}_3)_3$ aqueous solution. The X-ray absorption near edge structures (XANES) region is similar in both spectra. It shows a small prepeak followed by a sharp edge and a double peak. Since the crystalline hydrate shows long-range order, all features appear better resolved in the solid sample. Nevertheless, both spectra look similar, thus indicating that the local coordination environments are also similar; that is, the first coordination polyhedron around the Cr^{3+} ions is almost the same in the solid as in the aqueous solutions, both in number and type of neighbors and in local geometry.²⁹ Moreover, the fact that the amplitude of the EXAFS signal is similar in both cases indicates

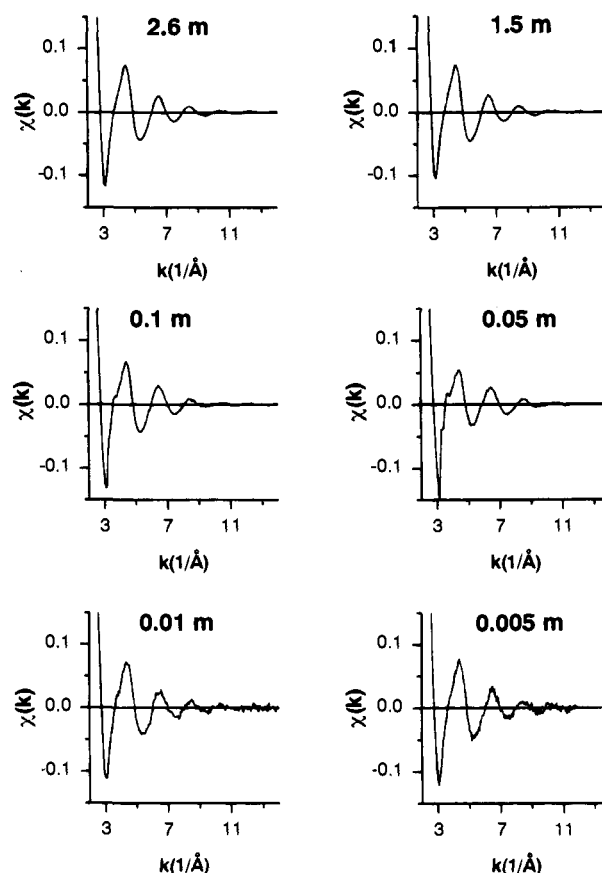


Figure 3. Raw EXAFS spectra at the Cr K-edge of $\text{Cr}(\text{NO}_3)_3$ aqueous solutions at different concentrations.

that the dynamic disorder is small in the solution, thus reflecting a high kinetic stability of the species responsible for the spectrum.

Figure 3 shows the unfiltered EXAFS raw data of the 2.6, 1.5, 0.1, 0.05, 0.01, and 0.005 *m* Cr^{3+} aqueous solutions, as obtained after pre-edge and background subtraction and normalization. The data quality is quite good except for the case of the solutions with concentrations 0.01 and 0.005 *m*, measured in the fluorescence mode, for which the signal to noise ratio is rather poor above $k = 10 \text{ \AA}^{-1}$. Nevertheless, taking into account that the expected contributions are from low *Z* scatterers, *i.e.*, oxygen atoms from water molecules, the intensity of the signal for higher values of energy is small, as shown in the other spectra in the same figure.

The absolute value and imaginary part of the phase-corrected Fourier transform of the EXAFS spectrum of the most concentrated solution, 2.6 *m*, and those of 0.01 *m* are plotted in Figure 4 ($\Delta k = 2.8\text{--}11 \text{ \AA}^{-1}$, k^2). Two peaks appear in these radial distribution functions. The first and most intense, centered at 2.0 \AA , superimposes in both solutions. The second, centered at around 4.0 \AA , is slightly shifted to a higher distance in the 0.01 *m* solution.

The data quality was good enough to analyze the unfiltered EXAFS spectra in the most concentrated solutions (2.6 and 1.5 *m*), while Fourier-filtered spectra were used for the other solutions. Parameters obtained from the fit of these spectra are included in Table 1. The fit weighting was 2 in all cases, and the quality of the fit was quantitatively indicated by the goodness of the fit values, ϵ_v^2 . The values of this parameter as well as the fit or Fourier filtering ranges and noise level appear in Table 2. The reliability of the fit is confirmed in the comparative plots in *k* and *R* space of the raw data and calculated EXAFS functions included in Figure 5 for the 2.6 *m* solution.

(34) Barwens, S. M. A. M.; van Zon F. B. M.; van Dijk, M. P.; van der Kraan, A. M.; de Beer, V. H. J.; van Veen, J. A. R.; Konningsberger, D. C. *J. Catal.* **1994**, *146*, 375.

Table 1. EXAFS Parameters of the $\text{Cr}(\text{NO}_3)_3$ Aqueous Solutions^a

$[\text{Cr}^{3+}]/m$	Cr-O shell	N	$R/\text{Å}$	$\Delta\sigma^2/\text{Å}^2$	$\Delta E_0/\text{eV}$
2.60	1st	6.4 ± 0.1	2.01 ± 0.008	0.0000 ± 0.0003	-0.8 ± 0.2
	2nd	13.1 ± 0.9	3.95 ± 0.06	0.009 ± 0.002	1.0 ± 0.6
1.5	1st	6.4 ± 0.1	2.01 ± 0.008	0.0000 ± 0.0003	-0.8 ± 0.2
	2nd	13.1 ± 0.8	3.95 ± 0.05	0.008 ± 0.002	1.0 ± 0.5
0.1	1st	6.1 ± 0.1	2.00 ± 0.01	0.0000 ± 0.0004	1.1 ± 0.3
	2nd	13.6 ± 1.4	3.96 ± 0.08	0.011 ± 0.003	1.1 ± 0.8
0.05	1st	6.0 ± 0.1	2.00 ± 0.01	0.0012 ± 0.0004	2.0 ± 0.3
	2nd	13.4 ± 1.3	3.97 ± 0.08	0.014 ± 0.004	1.0 ± 0.9
0.01	1st	6.0 ± 0.1	2.01 ± 0.01	0.0000 ± 0.0004	1.2 ± 0.3
	2nd	13.5 ± 1.2	4.02 ± 0.08	0.011 ± 0.003	1.0 ± 0.7
0.005	1st	6.4 ± 0.1	2.01 ± 0.01	0.0000 ± 0.0003	0.1 ± 0.3
	2nd	13.6 ± 1.0	4.00 ± 0.08	0.008 ± 0.003	0.0 ± 0.6

^a N , coordination number; $\Delta\sigma^2$, Debye-Waller factor; R , Cr-O distance; ΔE_0 , inner potential correction.

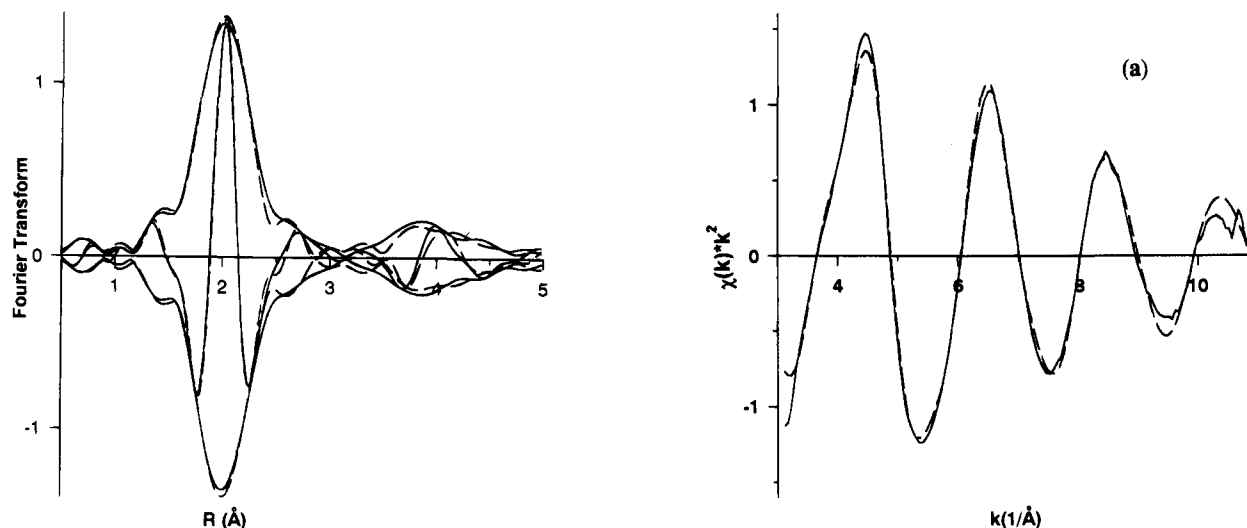


Figure 4. Absolute value and imaginary part of the phase-corrected Fourier transform of the EXAFS spectra of two $\text{Cr}(\text{NO}_3)_3$ solutions: 2.6 m (solid line) and 0.01 m (dashed line) ($\Delta k = 2.8-11 \text{ Å}^{-1}$, k^2).

Table 2. Fourier Filtering and Analysis Ranges, ϵ_r^2 , Goodness of Fit Values, and ν , Degrees of Freedom, for $\text{Cr}(\text{NO}_3)_3$ Aqueous Solutions of the Indicated Concentrations

$[\text{Cr}^{3+}]/m$	Fourier filtering		analysis range $\Delta k/\text{Å}^{-1}$	noise amplitude	ϵ_r^2	ν
	$\Delta k/\text{Å}^{-1}$	$\Delta R/\text{Å}$				
2.60			3.15-11	0.002	9.2	19.5
1.5			3.2-11	0.002	4.6	19.4
0.10	2.8-13.6	0.14-4.12	3.1-11.9	0.003	5.3	26.2
0.05	2.8-11.0	0.8-4.5	3.1-10.9	0.003	8.7	23.3
0.01	2.7-11.8	0.4-4.2	3-10.9	0.003	2.6	22.1
0.005	2.8-10.6	0.35-4.2	3-10.5	0.003	4.2	18.7

When the spectra of all the solutions are analyzed, the existence of two shells is confirmed. The first appears at 2.00–2.01 Å (± 0.01), the coordination number being between 6.0 and 6.4 (± 0.1), while the second appears at 3.95 Å (± 0.06) for 2.6 and 1.5 m solutions and at 4.02 Å (± 0.08) for the 0.01 m solution, its coordination number being between 13.1 and 13.6 (± 1). For the intermediate concentrations the Cr-O_{II} distance takes an intermediate value (3.97 Å). Debye-Waller factors, relative to the crystalline hydrate, are zero for the first shell in all solutions, and inner potential corrections range between -0.8 and $+2$ eV. For the second shell, Debye-Waller factors are considerably higher than for the first shell, as expected for the higher disorder. Inner potential corrections for the second shell remain similar to those of the first shell, ranging between 0.0 and 1.0 eV.

The detection of a second hydration shell is consistent with the findings of previous studies by X-ray diffraction (XRD) of

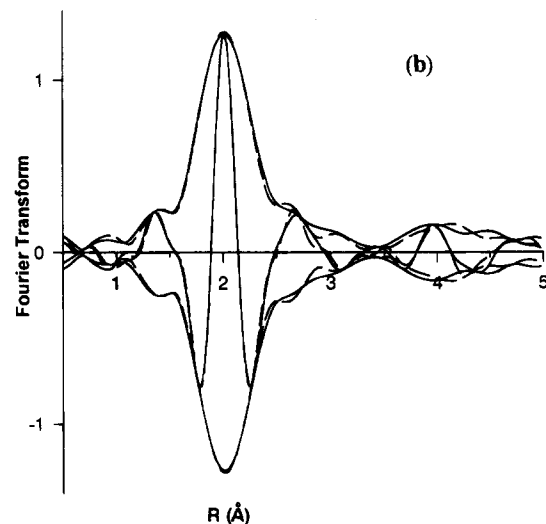


Figure 5. (a) Best fit (dashed line) and raw data (solid line) of the 2.6 m $\text{Cr}(\text{NO}_3)_3$ aqueous solution in k space ($\Delta k = 3.15-11 \text{ Å}^{-1}$). (b) Phase-corrected Fourier transform of the curves included in (a).

$\text{Cr}(\text{NO}_3)_3$ solutions, which led to the conclusion that the first-neighbor model was inadequate to describe the structure of the solutions considered.³⁵ These XRD data were only consistent with a model in which the hydrated ions $\text{Cr}(\text{H}_2\text{O})_6^{3+}$ interact strongly with a second shell of water molecules. This distribution corresponds to the concentric shell model proposed by

(35) Caminiti, R.; Licheri, G.; Piccaluga, G.; Pinna, G. *Chem. Phys.* **1977**, *19*, 371. Caminiti, R.; Licheri, G.; Piccaluga, G.; Pinna, G. *J. Chem. Phys.* **1978**, *69*, 1.

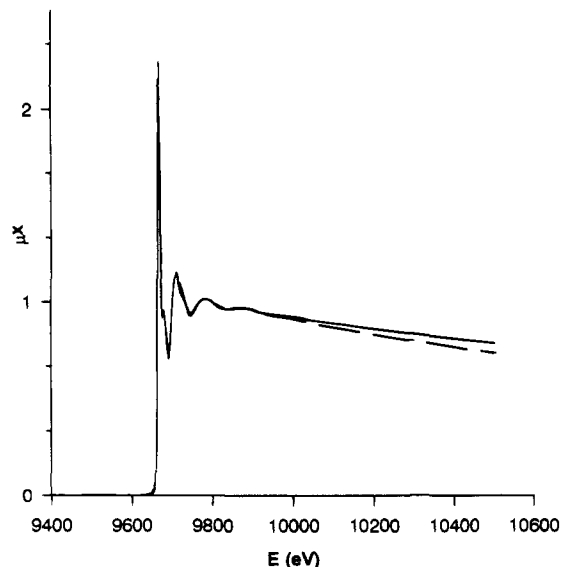


Figure 6. Normalized Zn K-edge absorption spectra of the crystalline hydrate $\text{Zn}(\text{NO}_3)_2$ (solid line) and the 0.1 *m* aqueous solution of the same salt (dashed line).

Frank and Evans,³⁶ according to which the hydration structure around metallic ions goes beyond the first hydration sphere.

It is important to remember that the accuracy of coordination numbers obtained by EXAFS is not high, and that indetermina-tion could be as high as 10%. Nevertheless, the signal to noise ratio in these spectra is quite good and data analysis is straightforward since there are only two contributions that are not interfering because they are separated by 2 Å; therefore, they can be analyzed with high precision. During the fitting procedure all parameters were left free, and in contrast to the procedure followed in the analysis of the XRD data, a coordination number of 6 for the first shell was not assumed during the analysis.

As observed in Table 1, the first hydration sphere is equal in all solutions, and the small differences observed can be attributed to small differences in data quality and not to structural differences between solutions, keeping in mind that the mea-surement of 0.05 and 0.005 *m* solutions was carried out at the limit of the transmission and fluorescence techniques, respec-tively. Although the amplitude of the signal is smaller and, thus, standard deviations are higher in the second hydration sphere, significant changes can be observed in the coordination distance: within the range of concentrations investigated, a contraction in the second hydration shell is observed with the increase of concentration. Differences in coordination numbers are within standard deviations in the calculation of this parameter.

4.2. Zinc Solutions. Figure 6 shows the low-energy part of the normalized Zn K-edge absorption spectra of the crystalline hydrate $\text{Zn}(\text{NO}_3)_2 \cdot 6\text{H}_2\text{O}$ and that of the 0.1 *m* Zn^{2+} aqueous solutions. As observed in Cr K-edge, both spectra are similar, the only difference being that the features appear more defined in the crystalline hydrate, as expected when a system with a long-range order is compared to a solution. As in chromium spectra, the similitude between the two spectra points to the existence of similar coordination polyhedra around the absorbing atom in both cases.

Figure 7 includes the *k*-weighted raw EXAFS spectra of Zn^{2+} aqueous solutions of concentrations 2.7, 1.1, 0.54, 0.1, 0.05, 0.01, and 0.005 *m*, obtained after submitting the above absorp-tion spectra to pre-edge and background subtraction and

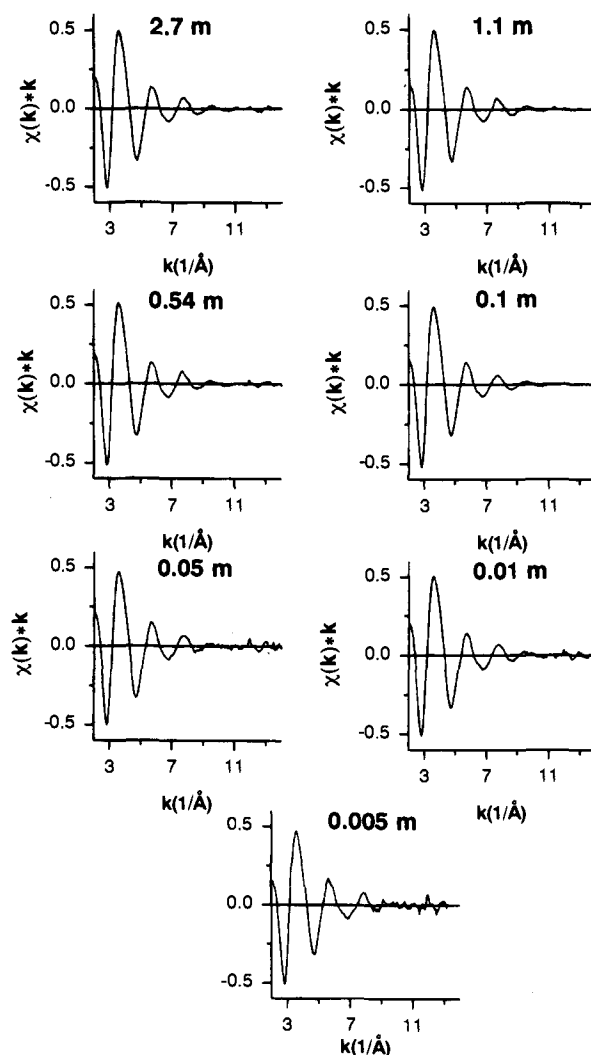


Figure 7. *k* weighted raw EXAFS spectra at the Zn K-edge of $\text{Zn}(\text{NO}_3)_2$ aqueous solutions at different concentrations.

normalization. No significant differences are found among these spectra, the main one being the noise level. The amplitude of the signal and the node positions are similar in all samples, and in fact, all spectra are nearly superimposed when plotted together. As expected, the high-frequency noise amplitude decreases with concentration, the most dilute solution presenting the worst signal/noise ratio. The similarities among all these spectra are clearly seen in Figure 8 including the absolute part of the Fourier transform of the EXAFS signals of four selected solutions that show a clear maximum centered at 2.05 Å in all of them. When comparing the raw EXAFS data of Zn^{2+} aqueous solutions, included in Figure 7 with those of Cr^{3+} , in Figure 3, it can be seen that the amplitude of the signal is smaller for Zn^{2+} solutions, even though these spectra are *k*-weighted. This was observed previously by Watanabe and co-workers³⁷ who have related it to different kinetic stabilities of the metal aquo complexes.

As in chromium solutions, data analysis is straightforward and even easier, since a reasonable fit can be achieved with a unique shell model. The inclusion of a second shell, which would correspond to a concentric shell model as in the case of chromium, improves the fit, as expected after doubling the number of free parameters. The degrees of freedom, *v*, after the inclusion of this shell is still quite high (higher than 20 in

(36) Frank, H. S.; Evans, M. W. *J. Chem. Phys.* **1945**, *13*, 507.

(37) Miyanaga, T.; Sakane, H.; Watanabe, I. *Bull. Chem. Soc. Jpn.* **1995**, *68*, 819.

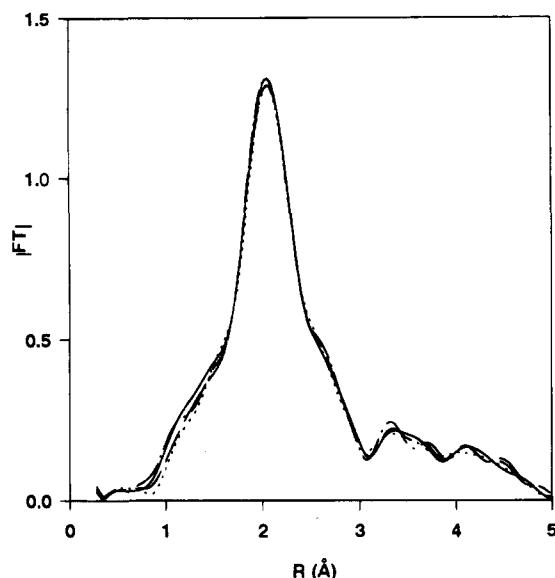


Figure 8. Absolute part of the phase-corrected Fourier transform of the EXAFS spectra for the following $\text{Zn}(\text{NO}_3)_2$ aqueous solutions: 1.1 m (—), 0.54 m (---), 0.1 m (···), 0.01 m (-·-·) ($\Delta k = 2.4\text{--}11.7 \text{ \AA}^{-1}$, k^2).

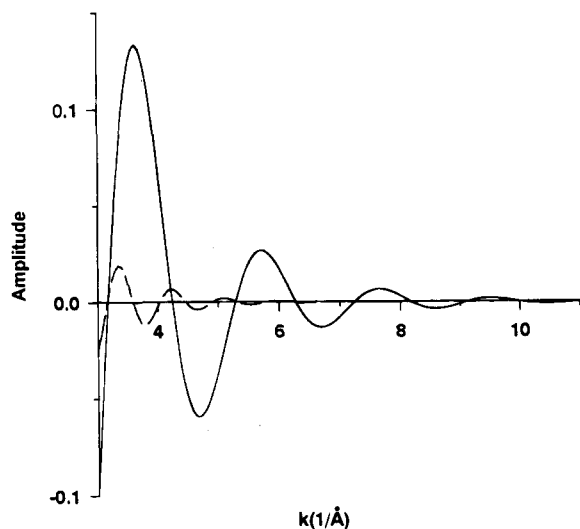


Figure 9. Calculated contribution with the parameters included in Table 3 for the first (solid line) and second (dashed line) hydration shells of a 0.1 m $\text{Zn}(\text{NO}_3)_2$ aqueous solution.

all cases), but it should be remarked that this shell is a minor contribution in the spectrum, its intensity being considerably smaller than that in the chromium solutions. Nevertheless, the amplitude of this signal is still higher than the noise level up to k values of 7 \AA^{-1} in all samples, as plotted in Figure 9, which includes the first and the second hydration shells calculated for the 0.1 m zinc solution (the maximum amplitude of the noise level, 0.001, superimposes the x axis).

Fitting parameters with their corresponding standard deviations appear in Table 3, while fitting ranges, the noise amplitude, degrees of freedom, and goodness of fit values are included in Table 4. Due to the excellent data quality, the unfiltered spectra have been analyzed, the fit weight being 2. The obtained goodness of fit values, ϵ_r^2 , are close to 1 in all cases (between 1.7 and 4.4) thus indicating that a good reproduction of the experimental spectra has been attained with the two shells fit. Additionally, the quality of the fit can be verified in the comparative plots included in Figure 10 of the best fit and raw EXAFS data in k and R space of the 0.1 m Zn^{2+} solution. Since

Table 3. EXAFS Parameters of the $\text{Zn}(\text{NO}_3)_2$ Aqueous Solutions^a

$[\text{Zn}^{2+}]/m$	Zn-O shell	N	$R/\text{\AA}$	$\Delta\sigma^2/\text{\AA}^2$	$\Delta E_0/\text{eV}$
2.70	1st	6.0 ± 0.1	2.06 ± 0.01	0.0097 ± 0.0004	1.4 ± 0.2
	2nd	6.7 ± 0.7	4.2 ± 0.2	0.021 ± 0.005	-4.0 ± 0.8
1.1	1st	6.0 ± 0.1	2.06 ± 0.01	0.0093 ± 0.0004	1.4 ± 0.2
	2nd	12.4 ± 1.6	4.1 ± 0.2	0.038 ± 0.007	-0.8 ± 0.9
0.54	1st	6.0 ± 0.1	2.05 ± 0.01	0.0094 ± 0.0004	1.5 ± 0.2
	2nd	11.8 ± 1.4	4.1 ± 0.2	0.040 ± 0.007	-0.9 ± 1.0
0.10	1st	6.0 ± 0.1	2.06 ± 0.01	0.0098 ± 0.0004	1.4 ± 0.2
	2nd	11.2 ± 1.4	4.1 ± 0.2	0.038 ± 0.007	-1.1 ± 1.0
0.05	1st	6.0 ± 0.1	2.05 ± 0.02	0.0097 ± 0.0004	1.8 ± 0.2
	2nd	11.2 ± 1.6	4.1 ± 0.2	0.039 ± 0.009	-2.0 ± 1.2
0.01	1st	6.0 ± 0.1	2.05 ± 0.02	0.0093 ± 0.0005	1.7 ± 0.2
	2nd	11.9 ± 1.9	4.1 ± 0.2	0.039 ± 0.009	-1.9 ± 1.2
0.005	1st	5.9 ± 0.1	2.05 ± 0.02	0.0098 ± 0.0006	2.0 ± 0.3
	2nd	11.2 ± 2.0	4.1 ± 0.3	0.041 ± 0.011	-2.0 ± 1.5

^a N , coordination number; $\Delta\sigma^2$, Debye-Waller factor; R , Zn-O distance; ΔE_0 , inner potential correction.

Table 4. Fourier Filtering and Analysis Ranges, ϵ_r^2 , Goodness of Fit Values, and ν , Degrees of Freedom, for $\text{Zn}(\text{NO}_3)_2$ Aqueous Solutions of the Indicated Concentrations

$[\text{Zn}^{2+}]/m$	analysis range $\Delta k/\text{\AA}^{-1}$	noise amplitude	ϵ_r^2	ν
2.70	3.10–11.7	0.0020	2.20	21.5
1.10	3.10–11.7	0.0020	4.40	21.5
0.54	3.10–11.7	0.0020	2.40	21.5
0.10	3.10–11.7	0.0020	2.20	21.5
0.05	3.10–10.0	0.0025	1.97	21.5
0.01	3.10–11.7	0.0025	2.00	21.5
0.005	3.10–10.7	0.0030	1.70	21.5

the spectra and EXAFS parameters are similar in the other cases, no more comparative plots have been included.

As anticipated from the comparative plots of the EXAFS spectra and radial distribution functions, fitting parameters are similar for all solutions, with the only exception of the second shell in the most concentrated one. For the first hydration shell, the coordination number is 6.0 in all samples (5.9 for the sample with 0.005 m concentration) and the standard deviation is 0.1. Debye-Waller factors ($\Delta\sigma^2$) range between 0.0093 and 0.0098 (± 0.0005), these values being similar to those reported from X-ray diffraction data, $\Delta\sigma = 0.1$.³⁸ The values of coordination distances, 2.05 \AA , are the same as those found in an EXAFS study of crystalline zinc hexahydrate and interlamellar hexahydrate intercalated in phyllosulfates.³⁹ This value is slightly smaller than the values reported by X-ray diffraction,⁶ 2.08–2.17 \AA . Inner potential correction values are similar in all cases, between 1.4 and 2.0 eV.

For the second hydration shell, the parameters obtained are similar with the exception of the more concentrated sample (2.7 m). The coordination number for the second shell is between 11.2 and 12.4, the coordination distance is *ca.* 4.1 \AA , and the inner potential correction ranges from -2.0 to -0.8 eV. For the most concentrated solution the best fit is achieved with a lower coordination number and Debye-Waller factor, and a longer distance. From XRD similar trends have been observed by Licheri *et al.*³⁸ who found a decrease in coordination numbers for the second hydration shell with concentration in a series of zinc sulfate solutions. The values reported by them are 12.5 for a 0.6 M solution, 9.9 for a 2 M solution, and 7.6 for a 3 M solution. As can be seen in Table 3, for all the other samples, the EXAFS parameters for this shell present similar values, the main difference being the increase of standard deviations in the most diluted solutions, as expected from the increase in the noise

(38) Licheri, G.; Paschina, G.; Piccaluga, G.; Pinna, G. *Z. Naturforsch.* **1982**, *37a*, 1205.

(39) Stoff, P.; Boulègue, J. *Am. Mineral.* **1988**, *73*, 1162.

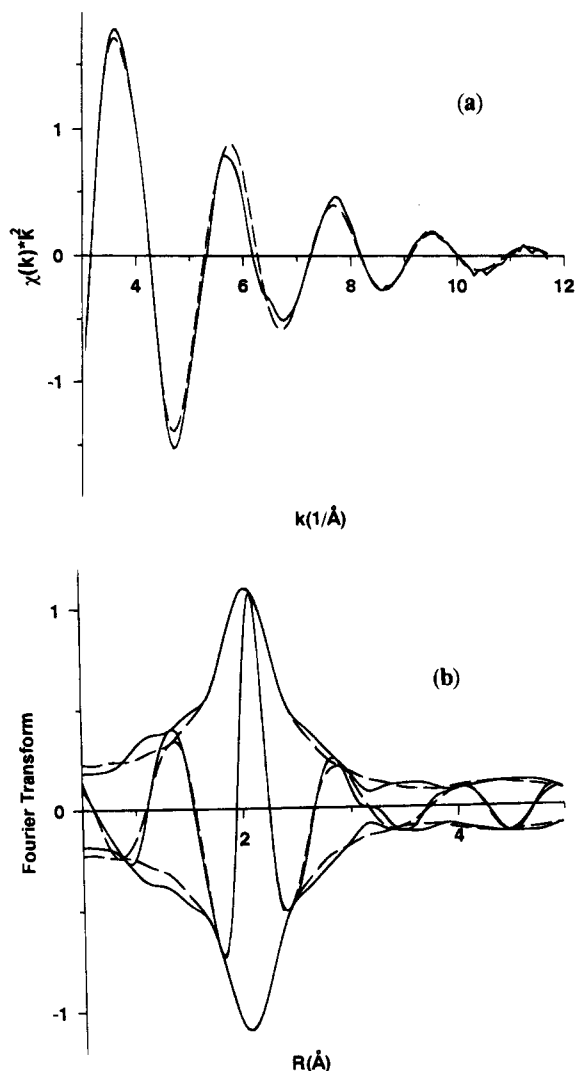


Figure 10. (a) Best fit (dashed line) and raw data (solid line) of the 0.1 *m* $\text{Zn}(\text{NO}_3)_2$ aqueous solution in *k* space ($\Delta k = 3.1\text{--}11.7 \text{ \AA}^{-1}$, k^2). (b) Phase-corrected Fourier transform of the curves includes in (a).

amplitude. The high value of the Debye–Waller factor, $\Delta\sigma^2 = 0.04$, rends the amplitude of this contribution much smaller than that of the corresponding second shell in chromium. Similar or even higher values have been reported from X-ray diffraction data ($\Delta\sigma = 0.06\text{--}0.16$),³⁸ while the values of the other parameters are consistent with previous results from XRD. No restrictions have been imposed during the fitting procedure, so that the values reported have been produced spontaneously by the fitting program from an eight-free-parameter fit. The same procedure has been followed for the seven spectra.

As explained in the Data Analysis, theoretical references have been used to fit the spectra of Zn^{2+} solutions because the crystalline hydrate presents a distorted octahedron in the first coordination sphere that rends its spectrum inadequate to obtain phase and back-scattering amplitude functions from it. Nevertheless, we have used the experimental spectrum of this compound of known structure to check the phase and back-scattering functions theoretically obtained. The crystalline structure of the solid hydrate has been determined by XRD,⁴⁰ the first coordination shell being formed by two Zn–O bonds at 2.064 Å, one Zn–O bond at 2.083 Å, one Zn–O bond at 2.104 Å, and two Zn–O bonds at 2.130 Å. We can describe the first coordination polyhedron either by a three-shell model,

$2 \times 2.064 + 2 \times 2.093 + 2 \times 2.130$, or by one shell formed by six Zn–O bonds at 2.095 Å.

We have fitted the first peak in the radial distribution function of the EXAFS spectra of the crystalline zinc hydrate using both models. A better fit was obtained with the second model: a single shell formed by 5.8 Zn–O bonds at 2.072 Å, the Debye–Waller factor being 0.0084 and the inner potential correction being 2.1 eV. The goodness of fit value, ϵ_0^2 , is 4.7, and the fitting range is $3.1\text{--}11.7 \text{ \AA}^{-1}$. When these values are compared with those of the crystalline hydrate, the obtained coordination number is 0.2 smaller, and coordination distances are 0.02 Å smaller. These values are exactly the standard deviations obtained for the corresponding parameters in the fit of the zinc solutions (± 0.1 and $\pm 0.01 \text{ \AA}$, respectively; see Table 3). On the other hand, the inner potential correction, 2.1 eV, is similar to the values obtained when fitting the solutions (values obtained range from 1.4 to 2.0 eV), and the Debye–Waller factor is lower than that of the solutions, as expected from the lower dynamic disorder of the solids. All these results confirm the suitability of the phase and back-scattering amplitude functions obtained theoretically.

5. Discussion

In 1988 Marcus said in his review⁴ about ionic radii in ionic solutions that, “...the application of EXAFS is still so recent and the amount of information gathered by it is still so scant that no great weight can as yet be placed on these results”. Things have changed remarkably since then, and provided the appropriate experimental devices are available, such as synchrotron sources, liquid EXAFS cells, fluorescence detectors, etc., EXAFS is a unique source of information for the geometric structure of dilute ionic solutions, as observed in the recent literature and in the results we present in this paper.

5.1. First Hydration Shell. From the analysis of the spectra of Cr^{3+} and Zn^{2+} solutions, we can conclude that the first hydration shell in both ions is formed by six water molecules at an average ion–oxygen distance of 2.00 and 2.05 Å, respectively. The Cr–O_I distance is similar to that obtained from X-ray diffraction data;^{4,6} reported values range from 1.97 to 2.03 Å, and the Zn–O_I distance is slightly smaller than the values obtained from the XRD data,^{4,6} 2.08–2.17 Å. Watanabe *et al.* by means of EXAFS found Cr–O_I distances of 2.03 Å^{29,41} and 1.98 Å⁴² for 1 and 0.1 M $\text{Cr}(\text{ClO}_4)_3$ aqueous solutions. When comparing our EXAFS data with XRD or neutron diffraction (ND) data, we have not observed, as Marcus did, a systematic decrease in distances of 1–2%. In fact, the average values provided in his review⁴ are 1.97 Å for Cr–O_I, shorter than our data, and 2.09 Å for Zn–O_I, longer than our distance.

The second conclusion obtained from the analysis of our data is that, within the concentration range studied, including from Debye–Huckel type solutions (0.005 *m*) to highly concentrated solutions (2.7 *m*), no significant changes are observed in the structural parameters of this shell, *R* and *N*, nor in the Debye–Waller factors, $\Delta\sigma^2$, or inner potential corrections values, ΔE_0 , for either ion. There is no other systematic study of the variation of the structure of the first hydration shell with concentration for Cr^{3+} aqueous solutions by XRD, ND or EXAFS. Only Caminiti *et al.*³⁵ studied 1.0 and 2.0 M $\text{Cr}(\text{NO}_3)_3$ solutions, but they did not report any systematic changes in distances or in Debye–Waller factors. As in other XRD studies, they assumed octahedral coordination, obtaining distances of 2.00 and 1.99 Å.

(41) Miyayama, T.; Watanabe, I.; Ikeda, S. *Chem. Lett.* **1988**, 1073.

(42) Sakane, H.; Miyayama, T.; Watanabe, I.; Matsubayashi, N.; Ikeda, S.; Yokoyama, Y. *Jpn. J. Appl. Phys.* **1993**, 32, 4641.

(40) Ferrari, A.; Braibanti, A.; Lanfredi, A. M. M.; Tiripicchio A. *Acc. Chem. Res.* **1967**, 22, 240.

Similarly, in all studies of the hydration structure of Zn^{2+} ions in aqueous oxyanion solutions, hexacoordination⁵ is assumed. One of these studies deals specifically with the dependence of the hydration parameters on the concentration of the solution.³⁸ In that work, five solutions of concentration ranging from 0.6 to 3.1 M were examined. The same model is consistent with all experimental data, and in the concentration range studied, no significant structural modifications were observed. The coordination distance, 2.13 Å, is slightly longer than the value found by us, 2.05 Å. Except for this difference, we conclude, as they did, that no significant structural modifications in the first hydration shell are observed within the range of concentrations studied. Nevertheless, we can extend this conclusion to concentrations 2 orders of magnitude smaller than they did (0.005 *m*). More recently, Watanabe and co-workers have carried out EXAFS measurements on 1 and 0.5 M Zn^{2+} aqueous solutions, obtaining Zn–O distances for the first shell of 2.13 Å^{29,41} and 2.08 Å⁴² without finding any changes in structural parameters with concentration.

Thus, it seems that the average structure of the closest environment to the cation is not modified with concentration, even when such a broad range of concentrations are considered. The ion–first hydration shell interactions are dominant in the determination of this structural parameter, and there is no discriminating role by changing the solvent molecules/counterions ratio of the solution.

The obvious advantage when using EXAFS as compared to XRD is that structural information can be obtained for highly dilute species, but EXAFS has the disadvantage of being highly sensitive to disorder. In fact, in this technique there is a second contribution to the Debye–Waller factor not present in XRD. For this technique one should consider the average value of the square of the displacement of an atom around its mean position, μ_0^2 , while for EXAFS the average of the square of the fluctuation of the distance between the central atom and the scatterer can be written as⁴³

$$\sigma_2^2 = \mu_0^2 + \mu_1^2 - 2\mu_0\mu_1 \quad (3)$$

μ_0^2 being the square of the displacement of the absorbing atom around its mean position and μ_1^2 the square of the displacement of the scatterer with respect to the absorbing atom. As a consequence, the EXAFS signal is sensitive to the kinetic stability of the bond between absorbing and neighboring atoms. However, the amplitude of the first hydration shell for both Cr^{3+} and Zn^{2+} ions is high enough to analyze this shell accurately, as shown by the small standard deviations in the structural parameters. In addition, our study provides a first estimate of the Debye–Waller factors that have to be correlated with the kinetic stability of aquo complexes. Thus, $[\text{Cr}(\text{H}_2\text{O})_6]^{3+}$ and $[\text{Zn}(\text{H}_2\text{O})_6]^{2+}$ have the same geometrical structure (six oxygens at around 2.0 Å), but they are species with very different kinetic stabilities and show different Debye–Waller factors in the first shell. Strong differences in these factors for the first hydration sphere have been found by Watanabe *et al.*³⁷ in an exhaustive study of the hydration structure of divalent and trivalent transition metal cations using EXAFS. They have correlated the observed differences with the kinetic stability of the aquo complexes, although they pointed out that the value of this factor is not affected by the real exchange motion of the ligand water molecule, but reflects the strength or stiffness of the atom–atom interaction. They have deduced a simple expression relating Debye–Waller factors and ligand exchange rate constants for metal ions in solutions. From this expression they

obtain a value for the frequency factor, *A*, in the Arrhenius equation, which coincides with that of a diffusion-controlled reaction. Although they have used the algorithm of McKale²⁶ to calculate the phase shift and back-scattering amplitude functions, while we used that of Rher²⁷ to calculate the Debye–Waller factors of Zn^{2+} solutions, we have obtained values similar to theirs, *i.e.*, 9×10^{-3} and 8×10^{-3} , respectively. In Cr^{3+} we have obtained these functions from an experimental spectrum, and thus we obtained only relative values that cannot be compared to the theoretical ones.

5.2. Second Hydration Shell. Confirming previous XRD and ND studies^{35,44,45} as well as our own work with EXAFS for several divalent and trivalent ion solutions^{7,46} and with Monte Carlo simulations for Zn^{2+} and Cr^{3+} solutions,⁴⁷ in all the solutions studied a second hydration shell is observed with an average of 12.5 neighbors (coordination number ranging from 11.2 to 13.6) at distances of *ca.* 4.0 Å for Cr^{3+} and 4.15 Å for the Zn^{2+} case. Due to the longer distance and higher disorder, the back-scattering amplitude in this second hydration shell is considerably smaller than that of the first hydration shell, particularly for the zinc case. As a consequence, higher indeterminism is found in the parameters of this shell. Nevertheless, even for Zn^{2+} solutions, the amplitude of this shell is higher than the noise level, as can be seen in Figure 9.

The small amplitude makes the ascription of this signal a matter of controversy. Moreover, in $[\text{Cr}(\text{H}_2\text{O})_6]^{3+}$ species, although water molecules in the first hydration shell are tightly bound with a mean residence time of days, this is not the case for water molecules in the second shell. The lower kinetic stability of $[\text{Zn}(\text{H}_2\text{O})_6]^{2+}$ should make the second hydration shell more disordered than in Cr^{3+} , and consequently it would show a higher Debye–Waller factor. In this sense, recent Monte Carlo simulations of the hexahydrate of Cr^{3+} and Zn^{2+} have shown that the RDF for hydrogen presents two peaks at the second hydration shell for the Zn^{2+} aqueous solution, but only one peak appears in the RDF of the Cr^{3+} solution.⁴⁸ Thus, if detected, this second shell is expected to show a smaller amplitude in the EXAFS spectrum than that corresponding to the Cr^{3+} aqueous solutions, as we have observed.

A second contribution at high *R* (*ca.* 4 Å) in the RDF of the EXAFS spectra of cationic aqueous solutions was detected by Benfatto *et al.*,⁴⁸ Sánchez del Río *et al.*,¹³ and more recently Filipponi.⁴⁹ All these authors have ascribed it to multiple scattering (MS) effects inside the octahedral cluster of the first hydration shell. Without neglecting the importance of MS effects, we think this ascription is not well founded since these authors discard “*a priori*” the existence of the second hydration shell. For instance, Sánchez del Río *et al.*¹³ state in their Introduction, “...*due to the structural disorder of the higher neighbours shells, the size of the effective absorbing cluster reduces to the first coordination shell*”. On the other hand, Filipponi *et al.*⁴⁹ in relation to the second peak of the EXAFS spectrum of Cu^{2+} aqueous solutions say that, “*the attempt to interpret this contribution as an additional single scattering*

(44) Bol, W.; Welzen, T. *Chem. Phys. Lett.* **1977**, *49*, 189.

(45) Dagnall, S. P.; Hague, D. N.; Towl, A. D. C. *J. Chem. Soc., Faraday Trans. 2* **1982**, *78*, 2161.

(46) Muñoz-Páez, A.; Díaz, S.; Pérez, P. J.; Martín-Zamora, M. E.; Martínez, J. M.; Pappalardo, R. R.; Sánchez Marcos, E. *Physica B* **1995**, *208–209*, 395.

(47) Pappalardo, R. R.; Sánchez Marcos, E. *J. Phys. Chem.* **1993**, *97*, 4500. Martínez, J. M.; Pappalardo, R. R.; Sánchez Marcos, E. *Proceedings of the VIIIth International Congress of Quantum Chemistry*; Academy of Sciences of the Czech Republic: Prague, 1994; p 365.

(48) Benfatto, M.; Natoli, C. R.; Bianconi, A.; García, J.; Marcelli, A.; Fanfoni, M.; Davoli, I. *Phys. Rev. B* **1986**, *34*, 5774.

(49) Filipponi, A.; D'Angelo, P.; Viorel Pavel, N.; Di Cicco, A. *Chem. Phys. Lett.* **1994**, *225*, 150.

signal would give completely unphysical results", referring to diffraction studies of other authors. But, although some diffraction and EXAFS studies of cupric aqueous solutions have not dealt with^{29,41,42,50-52} the second hydration shell, others have.⁵³⁻⁵⁵ In all the EXAFS studies ascribing the second peak in the RDF to MS effects, the initial assumption of the lack of order beyond the first hydration shell has not been reexamined. The success of this ascription is presumably due to the better quality of the fit obtained considering MS effects. Without considering the physical meaning of both hypotheses, there is an obvious reason for the better fit obtained when considering multiple scattering effects: there is a drastic increase in the number of free parameters, P . In our analysis the inclusion of a second shell adds four free parameters. When considering MS effects, a high⁵⁶ or unlimited⁵⁷ number of scattering paths, each with several (3-4) free parameters, are tested, the more relevant paths being included in the final fit, which obviously always improves. The increase in the number of free parameters, P , should imply a decrease in the degrees of freedom, ν , since the number of independent points, N_p , would remain constant. This should be reflected in the goodness of fit value, ϵ_v^2 , which would become worse in an apparent better fit. Nevertheless, the real improvement of the fit cannot be deduced from this parameter since authors using MS models do not show its value in their works.^{13,48,49}

An additional hypothesis suggested to explain the second peak in the Cr³⁺ spectrum is the existence of Cr³⁺ polynuclear aggregates. On the basis of EXAFS spectra of dimers implying Cr-Cr bonds, synthesized and trapped between the layers of a silicate,⁵⁸ this hypothesis can be discarded. In this system, although the coordination number for Cr-Cr bonds is small (average 1.0 for dimers and 1.5 for tetramers) its intensity is high enough to be clearly detected. In this system, the Cr-Cr distance is 3.2 Å, but the formation of such bonds has strong requirements of acidity, and dimer formation is a function of concentration. None of these conditions were fulfilled in our system: pH was equal to 1, the intensity of the peak did not decrease with concentration, and the distance Cr-Cr (3.2 Å) was much smaller than the value of the second peak (4 Å). Moreover, in our spectra the EXAFS function shows no significant oscillations for values of $k \geq 11 \text{ \AA}^{-1}$, which demonstrates that no significant Cr-high-Z element interactions are present and, hence, no Cr³⁺ polymeric species.

On the other hand, other groups with a long tradition in the experimental and theoretical study of ion solvation⁵⁹ have detected the second hydration shell by other techniques^{11,12} and have searched this shell, with the aid of EXAFS in the spectrum of a Rh³⁺ water solution, without finding evidence of this second

shell,¹⁰ presumably for reasons discussed in the Data Analysis, *i.e.*, that they discard meaningful information by restricting Δk ranges, particularly taking the minimum k value too high ($k \approx 4 \text{ \AA}^{-1}$).

Nevertheless, as explained in the Results, the existence of the second hydration shell for Cr³⁺ solutions was well established after the XRD studies performed by Caminiti *et al.*³⁵ of Cr(NO₃)₃ solution during the 1970s. These studies were the first case in which single scattering experiments supported unambiguously the existence of an ordered second coordination shell around the cation. The same conclusion was reached in subsequent studies of Cr(ClO₄)₃, CrCl₃, and Cr₂(SO₄)₃ aqueous solutions^{5,6}. Coordination distances found in these studies range from 4.00 to 4.25 Å, and coordination numbers from 10 to 14, although in a ND study of Broadbent *et al.*¹¹ using the first-order difference technique, they obtained a higher coordination number, 17-19.

Similarly, in an XRD study of Zn(SO₄)₂ solutions in a wide range of concentrations, Licheri *et al.*³⁸ observed in all the solutions a complex peak appearing at 4.10 Å, for which the most important contribution comes from the second shell. The same model was consistent with all experimental data, and in the concentration range studied, no significant structural modifications were observed. The only quantity that changed appreciably in their study was the second coordination number that decreased with increasing concentration as the number of available water molecules decreased.

Among all the possible ions, we chose the cations Cr³⁺ and Zn²⁺ because they have the same coordination polyhedra, a regular octahedron with M-O_l bond distances at $\sim 2.0 \text{ \AA}$, but they present different kinetic stabilities (the kinetic constant for water exchange rate $k = 3.2 \times 10^7 \text{ s}^{-1}$ for Zn²⁺ and $k = 5 \times 10^{-7} \text{ s}^{-1}$ for Cr³⁺).³ This difference is expected to drastically affect the Debye-Waller factor of the second hydration sphere for reasons similar to those for the Debye-Waller factor analyzed by Watanabe³⁷ for the first hydration shell, the strength or stiffness of the metal-oxygen bonds. On the other hand, as pointed out by Watanabe,⁶⁰ the less rigid structure of [Zn(H₂O)₆]²⁺ species compared to that of [Cr(H₂O)₆]³⁺ would damp out as well the MS contributions originating inside the first coordination polyhedra. But if the second peak were due to MS effects originating inside the first coordination cluster, we would expect this signal to be less affected by this kinetic factor than if the peak were due to the second hydration sphere. Thus, bearing in mind the above discussed reasons and the drastic differences observed in the back-scattering amplitudes of the second contribution to the EXAFS spectrum for these two ions, we discard the assignment of this contribution to MS effects inside the first coordination polyhedron. The MS hypothesis, although widespread, has many weak points, such as the inconsistency with the greater part of the diffraction studies carried out during the last 20 years. In good agreement with all these studies, and on the basis of the quality of our fit results, we explain these different back-scattering amplitudes as due to different Debye-Waller factors, which in turn reflect the different kinetic stabilities of the hexaquo complexes.

On the other hand, we have detected considerable MS effects in the solvated species formed in nonaqueous solutions of other transition metal ions, where the absorbing atom and at least two of the atoms of the solvent molecule are aligned; *i.e.*, the coordination or bond angle is close to 180°.⁶¹ Taking into account all these facts, we confirm our ascription of the second

(50) Beagley, B.; Eriksson, A.; Lindgren, J.; Persson, I.; Pettersson, L. G. M.; Sandström, M.; Wahlgren, U.; White, E. W. *J. Phys.: Condens. Matter* **1989**, *1*, 2395.

(51) Carrado, K.; Wasserman, S. R. *J. Am. Chem. Soc.* **1993**, *115*, 3394.

(52) Ohtaki, H.; Yamaguchi, T.; Maeda, M. *Bull. Chem. Soc. Jpn.* **1976**, *49*, 701.

(53) Magini, M. *Inorg. Chem.* **1982**, *21*, 1535.

(54) Musino, A.; Paschina, G.; Piccaluga, G.; Magini, M. *Inorg. Chem.* **1983**, *22*, 1184.

(55) Licheri, G.; Musino, A.; Paschina, G.; Piccaluga, G.; Sedda, A. F. *J. Chem. Phys.* **1984**, *80*, 5308.

(56) Mustre de León, J.; Rehr, J. J.; Zabinsky, S. I.; Albers, R. C. *Phys. Rev. B* **1991**, *44*, 4146.

(57) Filipponi, A.; Di Cicco, A.; Tyson, T. A.; Natoli, C. R. *Solid State Commun.* **1991**, *78*, 265.

(58) Bornholdt, K.; Corker, J. M.; Evans, J.; Rummey, J. M. *Inorg. Chem.* **1991**, *30*, 2.

(59) Akesson, R.; Pettersson, L. G. M.; Sandström, M.; Wahlgren, U. *J. Am. Chem. Soc.* **1994**, *116*, 8691, 8705.

(60) Watanabe, I. Personal communication.

(61) Muñoz-Páez, A.; Díaz, S.; Martínez, J. M.; Pappalardo, R. R.; Sánchez Marcos, E. To be published.

hydration peak in the RDF to a second hydration shell in Cr^{3+} and Zn^{2+} aqueous solutions. The smallest amplitude of this contribution in Zn^{2+} solutions produces higher standard deviations in the coordination parameters, which do not allow detection of significant differences in this shell with concentration. Thus, N varies between 12.4 and 11.2 with a standard deviation of 1.5, whereas the distances range from 4.12 to 4.22 Å, the standard deviation being 0.15 Å. A drastic change (50% reduction) is found in the coordination number for the most concentrated solution, 2.7 m , which reduces to 6.7. A similar change was observed by Licheri *et al.*³⁸ who explained it as due to the "deficit" in the number of water molecules available to coordinate Zn^{2+} ions, in this highly concentrated solution. The water molecules available, after discounting those used in the formation of the first hydration shell of Zn^{2+} ions have to be shared between NO_3^- ions and the formation of the second hydration shell. It seems that in the most concentrated solution the formation of this second shell suffers from this lack of water molecules. This fact is a confirmation of the ascription of this peak in the RDF to the second hydration shell.

The higher precision obtained in the study of Cr^{3+} solutions allows the detection of a contraction in the coordination distance of the second hydration shell with concentration (from 4.02 Å in the 0.01 m solution to 3.95 Å in 2.6 and 1.5 m solutions), the coordination number being similar in the range of concentration studied. Another difference when comparing Zn^{2+} with Cr^{3+} solutions is that a drastic decrease in coordination number in the most concentrated solutions of the latter was not detected. The reason for this difference may be the strongest interaction of Cr^{3+} ions, both with the first and the second hydration shells, which determines the preferential coordination of water molecules to Cr^{3+} ions and not to NO_3^- ions. Alternatively, the small changes detected in this shell for 2.6 and 1.5 m solutions (smaller distances and Debye-Waller factors) may be due to the inclusion of NO_3^- ions in the second coordination shell.

6. Conclusions

First Hydration Shell. As deduced from the analysis of their EXAFS spectra, the first hydration shell of Cr^{3+} and Zn^{2+} ions in aqueous solutions is formed by six water molecules at 2.00 and 2.05 Å, respectively. Within the wide range of concentration investigated (2.7–0.005 m), no significant systematic changes are detected in either type of solution, neither for metal–oxygen distances nor for coordination number. This seems to indicate that ion–ion interactions do not affect the structure of the first hydration shell of Cr^{3+} and Zn^{2+} ions.

Second Hydration Shell. Taking into account all the facts presented in the Discussion, we conclude that the additional contribution to the EXAFS spectrum observed in Cr^{3+} and Zn^{2+} aqueous solutions is due to the existence of a second hydration shell. The structural parameters (distance and coordination number) of this shell are similar to those obtained from neutron and X-ray diffraction studies and statistical simulations, 13.3 ± 1 neighbors at 4.0 Å for Cr^{3+} solutions and 11.6 ± 1.5 neighbors at 4.1 Å for Zn^{2+} . Contrary to that observed for the first shell, concentration seems to affect the structure in both types of solutions. For Cr^{3+} , the Cr–O_{II} distance lengthens with dilution. For Zn^{2+} solutions, the most concentrated solution (2.7 m) reduces its coordination number to *ca.* 7. The Debye-Waller factor is higher for Zn^{2+} solutions, as expected from the low kinetic stability of the $[\text{Zn}(\text{H}_2\text{O})_6]^{2+}$ species.

Acknowledgment. The Synchrotron Radiation Source at Daresbury Laboratories (U.K.) and the Large Installation Program-European Community are thanked for beamtime allocation, and the Dirección General de Investigación Científica y Técnica of Spain (Grant PB92-0671) is thanked for financial support. R.R.P. thanks the Ministerio de Educación y Ciencia for a postdoctoral contract.

JA951870X